Study on effects of highly deviated well on thin interbedded reservoirs fracturing

Han cheng [1, 2], Zaile Zhou [1, 2], Zhou Yun[1, 2], Zhiwen Li [3], Xianyin Qi [4]

[1] State key laboratory of geomechanics and geotechnical Engineering, Institute of Rock and Soil Mechanics, Chinese Academy of Sciences, Wuhan, Hubei 430071, China

[2] University of Chinese Academy of Sciences, Beijing 10049, China

[3] Institute of Oil and Gas technology, Changqing Oil Field Company of China National Petroleum Corporation, Xi'an, Shaanxi 710021, and China

[4] School of Urban Construction, Yangtze University, Jingzhou, Hubei434023; China

Abstract. Highly deviated well is widely applied in thin interbedded reservoirs fracturing in changqing oilfield. the oil production data shows that highly deviated fracturing well can increase the oil production compared with horizontal well fracturing, which suggests that highly deviated well fracturing is more efficient. However, it still needs deeper understanding for the mechanism of highly deviated well increase oil production, to study this problem, True-axial hydraulic fracturing physical simulation test is carried out on two kinds of cement specimen with interlayers, the results show that cement specimen for highly deviated well is more productive because fractures are more likely to cross the interbedded layers and connect oil reservoirs that separated by interlayers. Further research on the mechanism of highly deviated well fracture crossing interbedded layers is conducted via numerical simulation. Cohesive zone model is adopted to simulate the propagation of fracture in highly deviated well and horizontal well to compare the difference of thin interbedded layers stress. the results show that due to the deflection of highly deviated well fracture during propagation, the reservoir mass is divided into two parts, which causes relative displacement of rock mass on both sides of the fracture under the effect of vertical principal stress, thin interlayer eventually got broken under the action of tensile and shear stress. Both laboratory tests and numerical simulation results show that highly deviated wells have stronger interlayer penetration capability, which can improve the fracturing effect of thin interbedded reservoirs.

Keywords: Thin interbedded layers; Similarity model test; cohesive zone model; Crack propagation; highly deviated wells.

1. Introduction

In Changqing Oilfield, sandstone is the main oil-producing layer, and the main oil-producing layer is an ultra-low permeability unconventional reservoir with thin mudstone interlayers. When the researchers fracted this type of thin interlayer reservoir, they found that the oil production after fracturing of highly deviated wells by oilfield companies was significantly higher than that after fracturing horizontal wells. The transformation effect is better. When oilfield companies fracturing reservoirs with thin interlayers, the shape of hydraulic fractures is susceptible to differences in oil well inclination angle[3], in-situ stress[4], mechanics[5], and permeability[6] between thin interlayers and reservoirs Due to the influence of other factors, the actual expansion pattern in thin interlayer reservoirs is very complex, and researchers still lack a reasonable explanation for the mechanism of fracturing stimulation in thin interlayer highly deviated wells. Therefore, this paper studies the stimulation mechanism of thin interlayer fracturing, which provides new ideas and guiding significance for thin interlayer fracturing stimulation.

The fracturing effect of reservoirs with thin interlayers largely depends on the ability of hydraulic fractures to pass through thin interlayers. Oil and gas production has increased. Hou Bing [7] and others used sand-mud interbed samples to study the effect of directional fracturing fractures in inclined wells. They found that the perforation azimuth and the horizontal stress difference will directly affect the difficulty of fracture initiation. When the interlayer stress when the difference is

too large, the fracture will be blocked by the mudstone layer, which affects the propagation through the layer. Biot [8] believed that the difference in material mechanical properties between adjacent layers would have an impact on fracture propagation, and Biot gave the fracture penetration criterion under the condition of no fluid loss. Yang Zhaozhong [9] studied the factors of longitudinal expansion of hydraulic fractures in sand-coal interbeds based on pore-elasticity theory and damage mechanics. He found that the higher the viscosity of the fracturing fluid, the easier it is for hydraulic fractures to penetrate the sandstone layers, and the hydraulic fractures realize connectivity, which is consistent with the findings of Llanos [10]. Renshaw and Pollard [11] believed that the critical conditions for hydraulic fractures to penetrate layers are related to the maximum and minimum principal stress, rock tensile strength, and the friction coefficient of the interface layer. Based on the energy analysis method, Pan Rui [12] proposed that whether a hydraulic fracture can pass through a thin interlayer is related to the ratio of the fracture energy along the interface normal to the interface tangential. When the ratio is less than a certain limit, hydraulic fractures will pass through thin interlayers, which he verified with a cohesion element. The penetration process of hydraulic fractures involves the expansion of hydraulic fractures at the interface, and the interface properties are also an important factor affecting the results of penetration. Huang Rongzun [13] studied the interface strength. He believed that the interlayer interface strength is composed of the cohesion between the rock layers and the cohesion generated by friction. In the case of high interfacial cohesion, hydraulic fractures will penetrate through the layers. Enter the rock formation with smaller elastic modulus through the interface. Daneshy [14] believed that the interface property is an important factor affecting the vertical expansion height of reservoir fractures. The weakly cemented surface between layers will prevent the vertical expansion of fractures, and the weakly cemented surface between layers restricts the fractures in a single reservoir. Gao Jie [6] [15] used epoxy resin glue to simulate the bonding strength of sand-coal interlayer interface. He verified the rationality of the theory. He proposed that the relative strength of the interlayer interface and rock would also affect the vertical expansion height of cracks. Anderson [16], Teufel [17] and others studied the effect of interfacial friction on fracture propagation. They found that the higher the friction, the easier it is for hydraulic fractures to pass through the interlayer interface.

In general, the above studies focus on analyzing the interaction between planar hydraulic fractures and a single bedding interface, and the above studies seldom study the effect of non-planar propagation fractures on their ability to penetrate layers in highly deviated wells. Based on the low permeability sandstone reservoir in Huaqing Oilfield, this paper conducts true triaxial fracturing tests under the conditions of highly deviated wells and horizontal wells. This paper compares the ability of hydraulic fractures to penetrate layers to study the stimulation mechanism of highly deviated wells. In this paper, the pore pressure cohesion unit is further used to establish a numerical model of thin interlayer fracturing. The researchers simulate the interaction process of hydraulic fractures and thin interlayers under the fracturing conditions of highly deviated wells and horizontal wells. The researchers explain the stimulation mechanism of highly deviated wells.

2. Hydraulic fracturing model test

2.1. Development status of No. 6 reservoir in Changqing Oilfield which is affiliated to Huaqing Oilfield

Huaqing Oilfield is the main oil-producing area of Changqing Oilfield, and the No. 6 reservoir of Changqing Oilfield to which Huaqing Oilfield belongs is dominated by tight sandstone. The depth of the reservoir is 1970m~2160m, and there are two thin mudstone interlayers with a thickness of about 0.8m~1m in the reservoir. The researchers divided the sandstone reservoir into three parts, and the thickness of the middle sandstone reservoir was 30m~40m. Horizontal wells or highly deviated wells are often used to fracturing reservoirs, as shown in Figure 1. Figure 2 shows the obtained reservoir core samples, and the reservoir core samples include sandstone cores, mudstone cores and sand-mud interbedded cores. The researchers carried out mechanical and permeability parameter tests on the

reservoir core, and obtained the relevant parameters of the sandstone layer and the mudstone layer. As shown in Table 1.

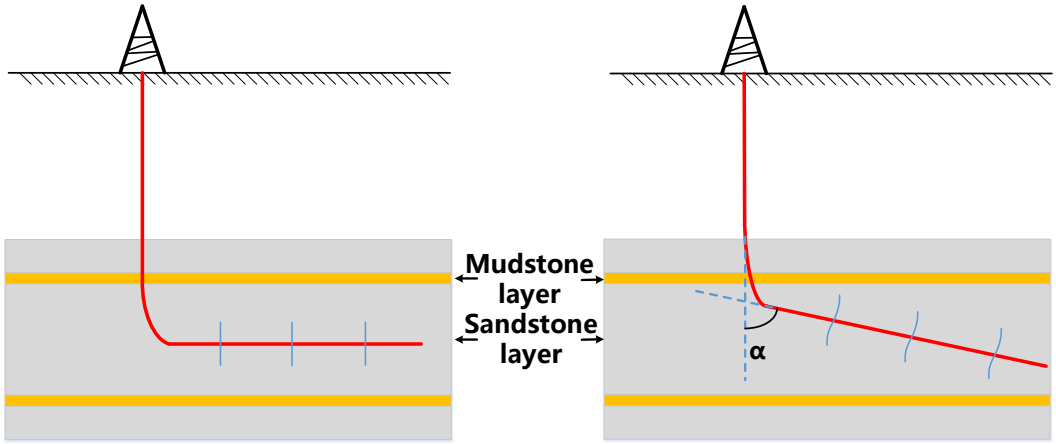

Fig 1. Geological conditions of Chang 6 reservoir.

(a) Sandstone core (b) Mudstone core (c) Sand-mud interbedded core

Fig 2. Chang 6 reservoir core.

Table 1. Material parameters for fracture zone.

	Elastic Modulus(GPa)	permeability coefficient(m/s)	Poisson's ratio	void ratio	Compression resistance(MPa)
sandstone layer	18.6	4×10^{-9}	0.15	0.08	80
mudstone formation	25.4	1×10^{-10}	0.16	0.08	55

2.2. Sample preparation and test equipment

According to the analysis of reservoir geological conditions in Huaqing Oilfield, the construction personnel used standard 42.5R ordinary black Portland cement to simulate sandstone reservoirs based on similar principles; the construction personnel used 32.5R white Portland cement to simulate thin mudstone interlayers. Both cements were mixed with quartz sand (40-80 mesh) at a mass ratio of 1:1 for pouring. The material parameters are shown in Table 2. In order to ensure the good delamination of the samples, the construction personnel inserted a separator into the mold during pouring (Fig. 3(a)). White cement was poured inside the separator to simulate the mudstone layer, and black cement was poured outside the separator to represent the sandstone reservoir. Pull out the partition when finished. Among them, the thickness of each thin interlayer is 20mm, and the overall size of the sample is 310×310×310mm. After the pouring is completed, the construction personnel maintain the fracturing pattern for 15 days. Figure 3(b) shows the fracturing sample after pouring. In order to facilitate the development of the subsequent fracturing test, the horizontal well casing and the highly deviated well casing are fixed in the middle black cement layer by pouring and pre-embedding. And the arrangement of thin interlayers is shown in Figure 4.

Table 2. Material parameters for cement.

Material name	Elastic Modulus/GPa	Poisson's ratio	Compression resistance/MPa
32.5RWhite cement	5.96	0.264	26.25
42.5Rblack cement	9.48	0.262	32.14

(a) Placing the partition plate (b) The actual cement sample

Fig 3. Cement sample for fracturing.

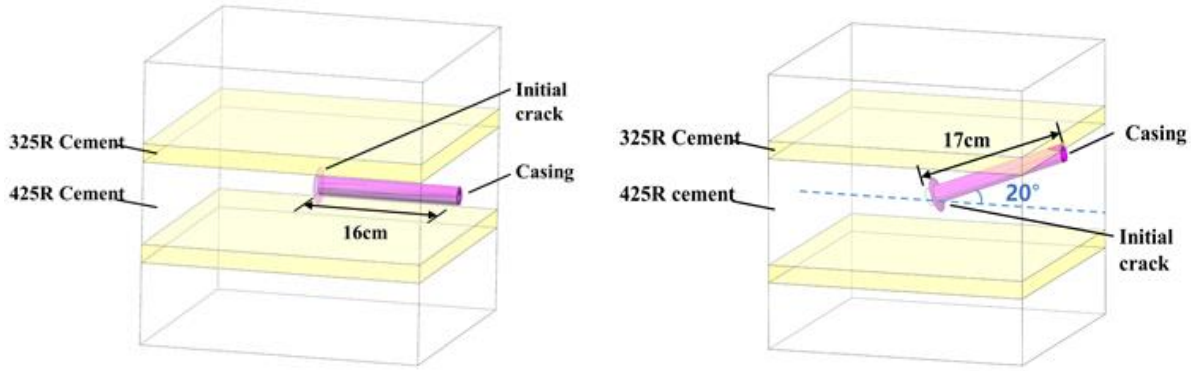

(a) Horizontal well (b) Highly deviated well

Fig 4. The structure of cement specimen.

2.3. Test process

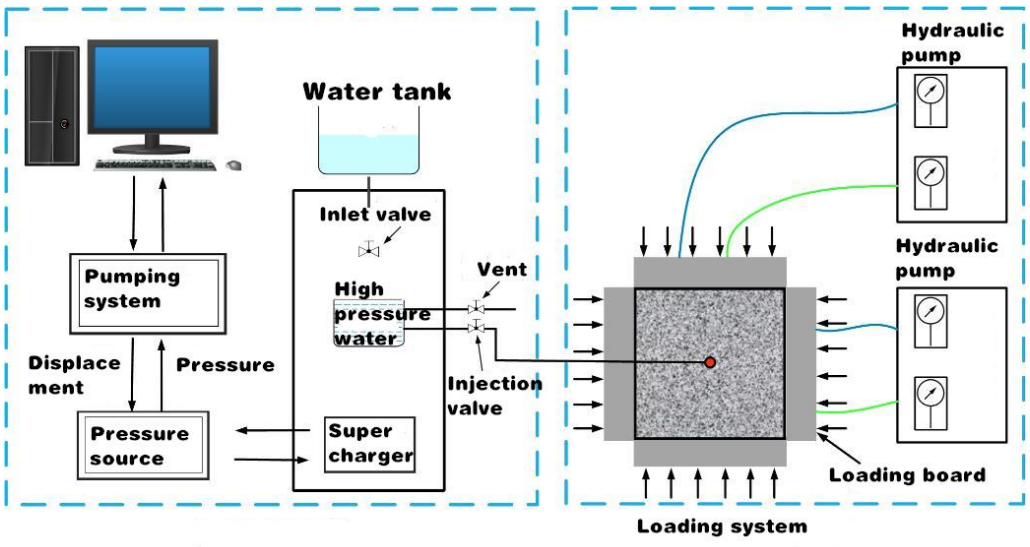

Fig 5. True tri-axial fracturing test system.

Figure 5 is a schematic diagram of the true triaxial hydraulic fracturing test system. The test system consists of a servo pump system and a loading system. For details of the equipment parameters, please refer to the literature [18] [19]. The fracturing test process is as follows:

2.3.1 Test for tightness of the sample. When the tester pours, it is inevitable that cracks will be formed when the diaphragm is poured in layers. Before the test, the tester needs to check the air tightness of the sample to ensure that the sample does not have cracks connecting to the outside world;

2.3.2 Marking and taking pictures. The experimenter draws the loading direction of the three-dimensional stress on each surface of the qualified fracturing sample, and the experimenter takes pictures to record the initial state of the sample;

2.3.3 Place the cement sample and the loading plate, and the experimenter connects the injection port of the servo hydraulic pump to the wellbore interface;

2.3.4 Loading triaxial stress. When loading, the experimenter first loads the confining pressure, and then loads the bias voltage, and the experimenter first loads the stress perpendicular to the layer direction;

2.3.5 The experimenter opens the water inlet valve and the exhaust valve, the experimenter waits for the high-pressure water tank to be full before closing it, the experimenter opens the injection valve, the experimenter starts the servo pump system, and the experimenter sets the injection rate of the fracturing fluid. The fracturing fluid is a certain concentration of guar gum. In order to make the fracture expansion pattern clearer, the experimenter added a red dye to the fracturing fluid as a tracer;

2.3.6 Disassemble the sample. When unloading, the experimenter unloads step by step; the experimenter cuts the sample and records it by taking pictures. The experimenter described the hydraulic fracture morphology according to the distribution of the dye to evaluate the fracturing effect of the sample.

According to the in-situ stress conditions of the No. 6 reservoir in Changqing Oilfield, the vertical in-situ stress is 50 MPa, the maximum horizontal in-situ stress is 40 MPa, and the minimum horizontal in-situ stress is 34 MPa. The actual loading in this paper reduces the three-dimensional stress by 4.2 times. The load order is $\sigma_v \rightarrow \sigma_H \rightarrow \sigma_h$ (Fig. 7), the experimenter loaded the triaxial stress to 8.16MPa, and then the experimenter loaded the bias voltage to the set value. The viscosity of the test fracturing fluid was 50 mPa·s, and the pumping rate was 0.01 l·min-1. The comparison of field conditions and fracturing model test parameters is shown in Table 3.

Natural Science Foundation.

Table 3. Parameters for hydraulic fracture model test.

Parameter	σ_v /Mpa	σ_H /MPa	σ_h /MPa	Fracturing fluid viscosity/(mPa·s)	Pumping rate /(l·min^{-1})
Test parameters	12	9.6	8.16	50	0.01
Field parameters	50	40	34	1.5	2000

2.4. Fracturing test results

Figures 6 and 7 are respectively the fracture morphology diagrams of horizontal wells and highly deviated wells. Figure 6 is the hydraulic fracture morphology drawn according to the red tracer, and Figure 7 is the schematic diagram of the fracture morphology drawn according to the tracer distribution.

Figures 6(a) and 7(a) are the results of the horizontal well fracturing test. The hydraulic fractures started at the initial fractures, and then deflected quickly after the fractures and expanded in the vertical direction. The angle passes through the interface between the middle layer and the upper and lower thin interlayers, and then the fracture reaches the surface of the sample. On the other side, the fracture turns along the interface between the upper reservoir and the upper thin interlayer after penetrating the thin interlayer (Fig. 7(a)), and then the fracture extended to the surface of the specimen. Under the fracturing conditions of horizontal wells, the fracture morphology is that hydraulic fractures are diverted at the interface between the upper reservoir and the upper thin interlayer, and the scope of reservoir fracturing is limited to the intermediate reservoir.

Fig. 6(b) and Fig. 7(b) are the fracturing test results of highly deviated wells. It can be seen that the hydraulic fractures are rapidly deflected to expand perpendicular to the direction after initiation

in the intermediate reservoir section, and the hydraulic fractures then maintain this direction. Extending to the thin interlayer, one wing of the fracture penetrates down the thin interlayer and still extends in a vertical direction, and finally the hydraulic fracture extends to the surface of the sample, and the other wing is captured at the upper reservoir and the upper thin interlayer (Fig. 7(b))). The fracture morphology of the highly deviated well fracturing test shows that the hydraulic fracture passes through the thin interlayer, and the hydraulic fracture connects the intermediate reservoir and the lower reservoir, and the fracturing area is significantly larger than that of the horizontal well. The fracturing test results show that under the same in-situ stress conditions, thin interlayer penetration occurs after fracturing in highly deviated wells. Therefore, laboratory tests show that the fracturing effect of highly deviated wells is better than that of horizontal wells.

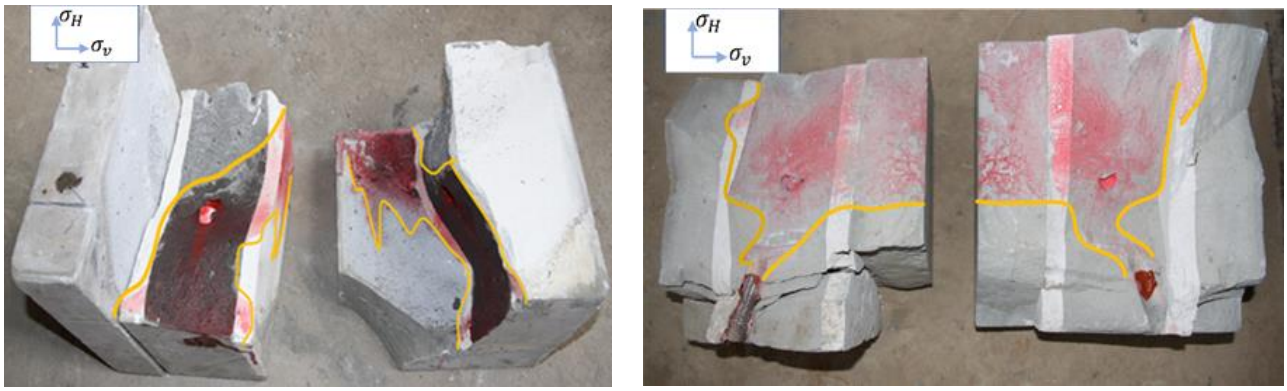

(a)Horizontal well (b)Highly deviated well

Fig 6. Crack propagation for horizontal well.

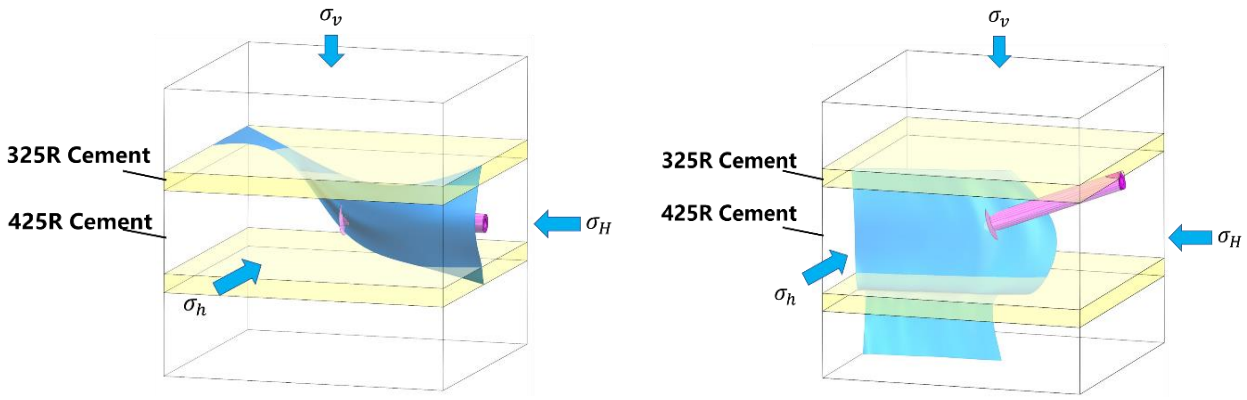

(a)Horizontal well (b)Highly deviated well

Fig 7. Crack propagation for fracture physical test.

3. Numerical simulation of hydraulic fracturing in reservoirs with thin interlayers

3.1. Cohesion unit verification

In order to further study the thin interlayer penetration mechanism under the fracturing condition of highly deviated wells, the researchers used the cohesion unit method to establish a thin interlayer fracturing model according to the rock mechanics parameters of the No. 6 reservoir in Changqing Oilfield.

First, the researchers verified the correctness of the cohesion element method to simulate the hydraulic fracturing problem based on the analytical solution of hydraulic fracturing. According to the theory of Detournay [20], the crack propagation results of the KGD model are related to the dimensionless fracture toughness. At that time, the hydraulic fracture propagation was mainly

controlled by viscosity. At that time, the hydraulic fracture propagation was mainly controlled by the fracture toughness of the rock mass. The formula is: $\kappa=\frac{K'}{(E'^3\mu' Q_0)^{\frac{1}{4}}}$

The expressions of parameters E', μ', K' are:

$$E'=\frac{E}{1-\nu^2},\quad \mu'=12\mu,\quad K'=4\sqrt{\frac{2}{\pi}}K_{IC} \tag{1}$$

In this expression, E is the elastic modulus of the rock mass, ν is the Poisson's ratio of the rock mass, and K_{IC} is the fracture toughness of the rock mass material.

Set the hydraulic fracture opening w (s, t) of the KGD model, the hydraulic fracture half-length l(t), the net pressure p(t) at the injection point of the fracture, and the calculation formula of ( ) under viscosity control is as follows [20]:

$$\left.\begin{aligned} p &= 0.545\left(\frac{\mu' E'^2}{t}\right)^{\frac{1}{3}} \\ w(x,t) &= 0.616\left(\frac{\mu' Q_0^3 t^4}{E'}\right)\left[1.732\left(1-\left(\frac{s}{l}\right)^2\right)^{\frac{2}{3}}-0.156\left(1-\left(\frac{s}{l}\right)^2\right)^{\frac{5}{3}}+0.0663\left[4\sqrt{1-\left(\frac{s}{l}\right)^2}+2\left(\frac{s}{l}\right)^2\ln\left|\frac{1-\sqrt{1-\left(\frac{s}{l}\right)^2}}{1+\sqrt{1-\left(\frac{s}{l}\right)^2}}\right|\right]\right] \\ l(t) &= 0.616\left(\frac{E' Q_0^3 t^4}{\mu'}\right)^{\frac{1}{6}} \end{aligned}\right\} \tag{2}$$

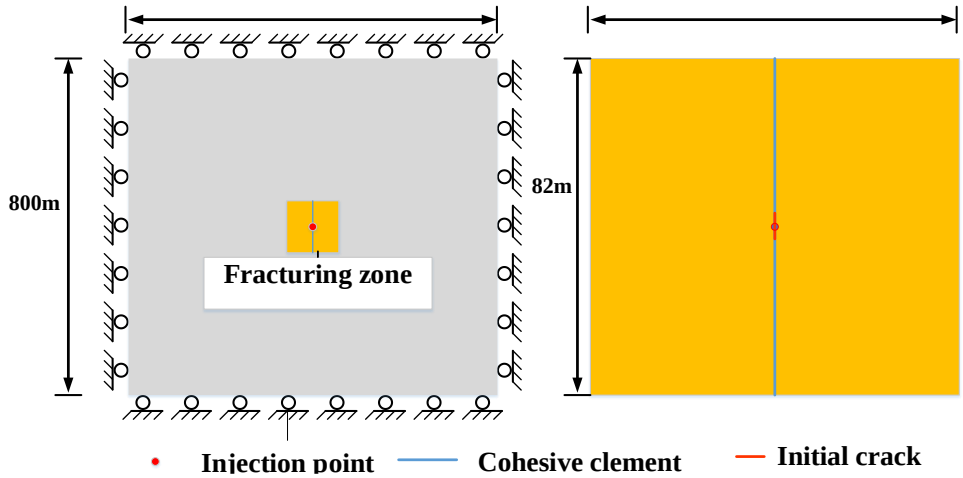

(a) Global view of the model (b) Enlarged view of the fracturing area.

Fig 8. Two-dimensional plane strain model.

The fracturing verification model of the cohesion unit is shown in Figure 8. The overall size is 800 × 800 m. The right picture is a partial enlarged view of the fracturing area, and its size is 82 × 82 m. The experimenter arranged an initial fracture with a length of 1 m in the center of the fracturing zone. The midpoint of the initial fracture was the injection point of the fracturing fluid. The fracturing fluid with a viscosity of 1 mPa s was injected. The pumping rate Q0 was 0.001 m2/s. The injection time is 100s; the rock elastic modulus E=18.6GPa, Poisson's ratio ν=0.15, fracture toughness KIC=3.54MPa·m1/2, the experimenter did not consider the filtration of fracturing fluid in the verification example, and the experimenter used CPE4 Elements characterize hydraulic fractures, and experimenters use structured grids to perform calculations. From the expression (1), the dimensionless fracture toughness of the model can be obtained κ = 0.665, which belongs to the viscosity-controlled hydraulic fracturing mode. Figure 9 shows the comparison between the

numerical solution of hydraulic fracturing based on the cohesion unit and the analytical solution of KGD viscosity control. The experimenters can see from the comparison results that, except for the slight jitter in the initial short-term (t<2s) pumping pressure, the pumping pressure in other ranges and the slit width at the injection point are in good agreement. When the pump injection time is 100s, the analytical solution of the injection point pressure is 1.922MPa, the corresponding numerical solution is 1.979MPa, and the relative error is 2.93%; the analytical and numerical solutions of the corresponding injection point fracture opening are 4.87×10-3m and 4.94×10-3m, the relative error is 0.98%, the calculation results verify the rationality of the cohesion element method to simulate the hydraulic fracturing problem.

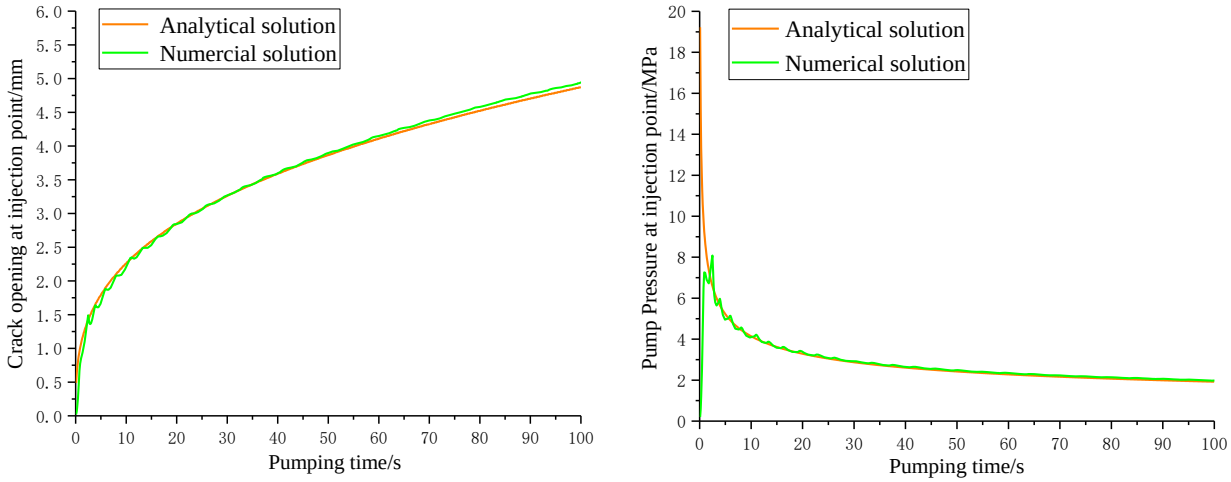

(a)Fracture opening at injection point (b)Injection point pressure

Fig 9. Viscosity dominated ($\kappa \leq 1$) Theoretical solutions and numerical solutions.

3.2. Interfacial shear strength of thin interlayers

The intersection of hydraulic fracture and thin interlayer interface may occur in three situations: penetration, migration, and capture (Fig. 10). The interfacial shear strength is the main controlling factor affecting the ability of hydraulic fractures to penetrate through layers [16]. The interfacial shear strength can be divided into two parts: the interlayer adhesion force and the interlayer friction force [21]. The researchers use the Mohr-Coulomb criterion to express it as: $\tau = \mu\sigma_n + C$ (4) where τ is the shear strength of the interface, is the normal stress perpendicular to the interface direction, is the coefficient of friction, and C is the cohesion between layers. In this paper, linear interpolation is used to estimate the shear strength of the material. In this paper, the direct shear test is carried out on the sandstone, mudstone, and sand-mud interbed cores obtained on site. In this paper, the Mohr-Coulomb formula is extrapolated to the shear strength under normal ground stress. The shear strength values of different cores are shown in Table 4 as the tangential damage strength of the cohesion unit.

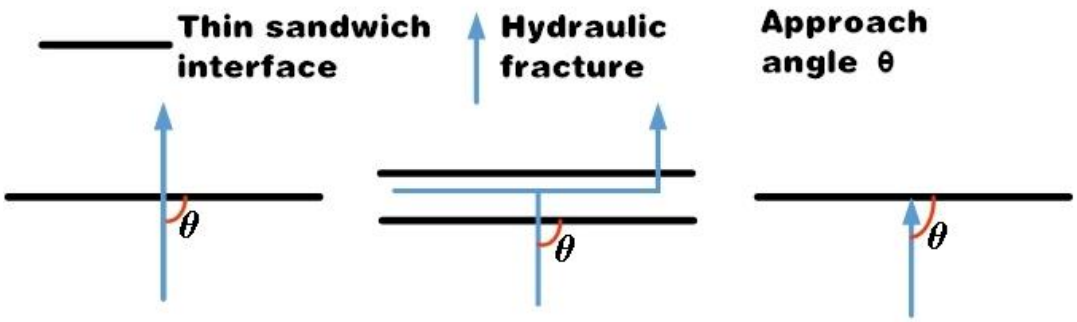

(a) Penetration (b) Offset (c) Capture

Fig 10. Three situations of hydraulic fracture intersecting with interlayer interface.

3.3. Fracturing model with thin sandwich

When simulating the interaction between hydraulic fractures and thin interlayers based on the pore pressure cohesion unit, this paper adopts the method of combining the degrees of freedom of the pore pressure unit to keep the pore pressure at the intersection point continuous, as shown in Figure 11. The four nodes of the element boundary (red nodes) have displacement degrees of freedom and pore pressure degrees of freedom, and the intermediate nodes (pink, yellow and blue nodes) have only pore pressure degrees of freedom. At the intersection, the four intermediate pore pressure nodes of the element are merged into a whole pressure node (blue node).

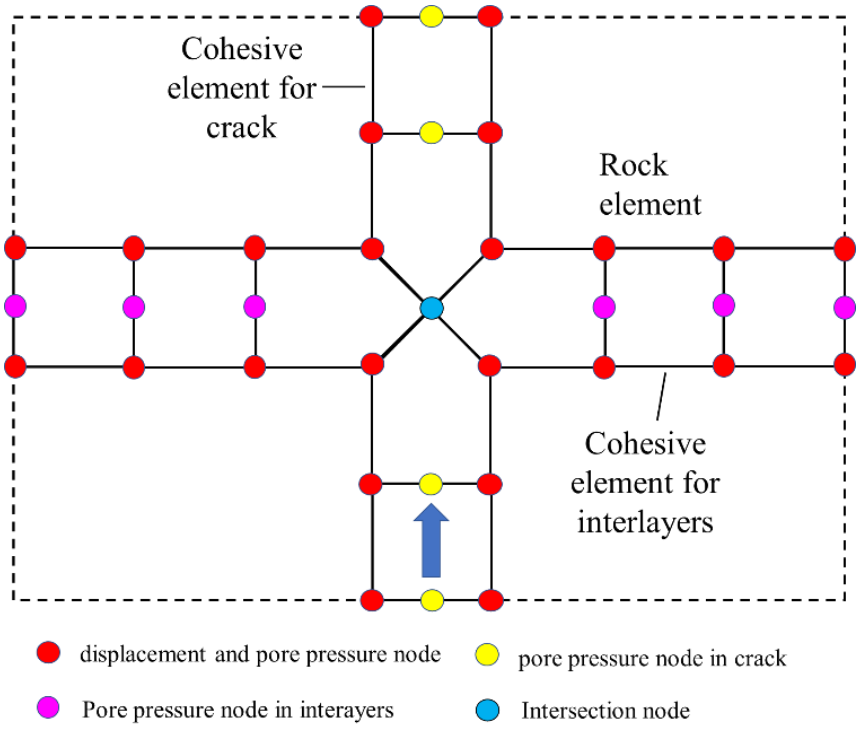

Fig 11. Interaction node in cohesive element.

Figure 12 is a simplified model of the fracturing zone, which simulates two well types of horizontal wells and highly deviated wells, and the other conditions are exactly the same. For the convenience of description, the experimenter calls the thin interlayer interface closest to the fracturing fluid injection point as the first (inner) interface, and the experimenter calls the thin interlayer interface farther from the injection point as the second (outer) interface (Fig. 13). In order to reduce the influence of boundary effects on the calculation results, the size of the global model is also set to 800×800m, and the size of the fracturing zone in the center of the model is 82×82m; The length of the fracturing section is 2m, and the injection point is located at the center of the fracturing zone, a distance from the thin interlayer. The first (inner) interface d is 20m, σ_{H} , σ_h , σ_v are the maximum horizontal, minimum horizontal and vertical ground stress, respectively, the directions are the same as the model coordinates Ox, Oy, and Oz axes, respectively, and the sizes are 40MPa, 34MPa, 50MPa Model boundary holes The pressure is set to 0; the loading conditions are divided into the in-situ stress balance analysis step and the fracturing fluid injection analysis step. The in-situ stress balance analysis step simulates the initial in-situ stress conditions in the fracturing area. In the fracturing fluid pump injection analysis step, the injection rate is 0.005m2/s, and the pumping time is 150s. The cohesion unit arrangement in the fracturing zone is shown in Figure 11. For horizontal wells, the experimenters consider that the perforation direction is always perpendicular to the wellbore axis, and the hydraulic fractures extend along the vertical in-situ stress (Oz) direction before intersecting the thin interlayer; The inclination angle of the well was set to 70°, the angle between the initial fracture and the vertical in-situ stress was set to 20°, the hydraulic fractures were gradually deflected along the initial fracture to the direction of the vertical in-situ stress, and the hydraulic fractures

formed curved and inclined fractures. In addition, according to the possible propagation of hydraulic fractures in thin interlayers, the experimenters also arranged cohesion elements at the interface of thin interlayers and on the possible extension paths of hydraulic fractures. Experimenters in the fracturing area used structured grids with a minimum unit size of 0.5m and a maximum unit size of 2m. The material parameters of the cohesion element are shown in Table 4.

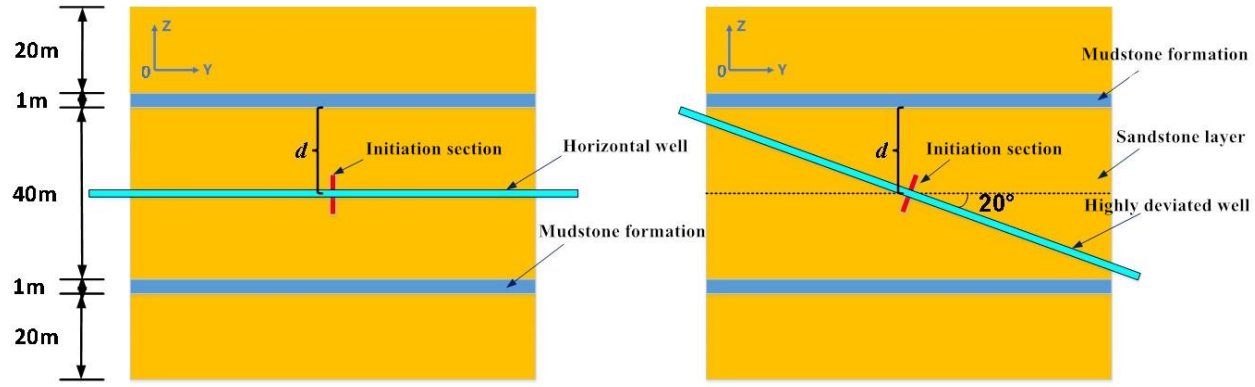

(a) Fracturing model for horizontal wells. (b) Fracturing model for highly deviated wells.

Fig 12. Simplified model for fracture zone.

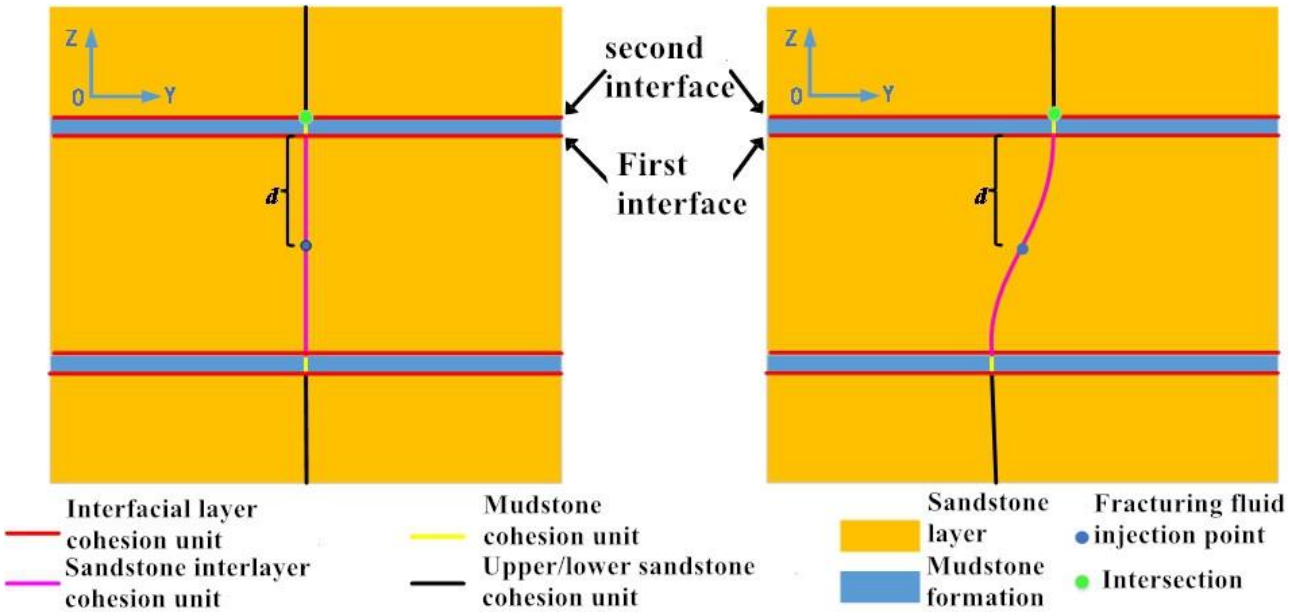

(a) Layout of cohesion units in horizontal wells. (b) Layout of cohesion units in highly deviated wells.

Fig 13. Distribution of cohesive element in fracture area.

Table 4. Parameters employed in cohesive elements.

Unit type	Normal critical energy release rate(Pa·m)	Initial crack stiffness(1×10^{13}N/m)	Normal damage strength(MPa)	Tangential damage strength(MPa)	Filter loss coefficient(m/min$^{0.5}$)
Sandstone upper/lower cohesion unit	800	9.3	8	42.9	1×10^{-15}
Mudstone cohesion unit	750	12.7	7.5	36.4	1×10^{-17}
Interfacial cohesion unit	200	11.2	2	25	1×10^{-14}
Sandstone Middle Cohesion Unit	650	9.3	6.5	40.49	1×10^{-15}

3.4. Fracturing simulation results

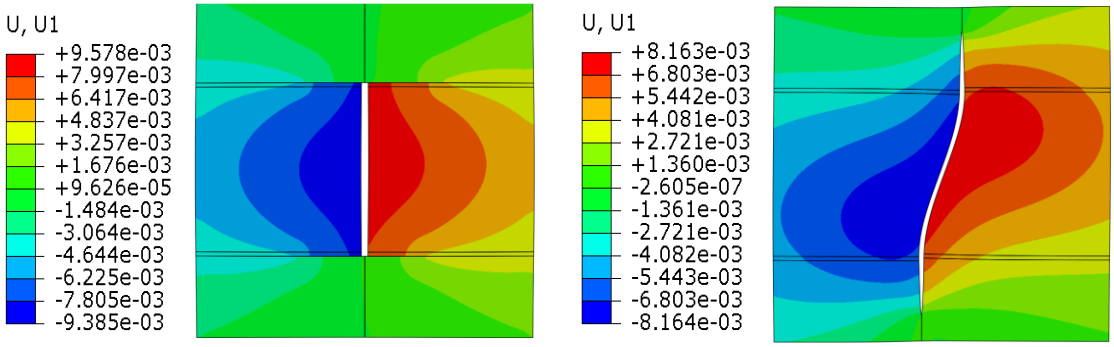

(a) Horizontal displacement for horizontal well.(b) Horizontal displacement for highly deviated well.

Fig 14. Contour for fracturing horizontal displacement.

Figure 14 shows the shape of the fracture after stable expansion (t=150s). After the horizontal well initiated fracture passes through the first interface, the fracture is captured at the second interface. With the continuous injection of fracturing fluid, the fracture begins to laterally Expansion, the scope of fracture stimulation is limited to the middle reservoir, the fractures of the highly deviated well penetrated the thin interlayer, and the fractures entered the top and bottom reservoirs, and the three reservoirs divided by the thin interlayer were all stimulated. Larger than horizontal wells.

In order to analyze the reason why the fractures in highly deviated wells have stronger ability to penetrate through layers, the experimenters extracted the stress-time curve (Fig. 15) of the intersection of hydraulic fractures and the second interface (Fig. 13) in horizontal wells and highly deviated wells. Figure 15(a) is the comparison curve of tensile stress at the intersection point. The two curves have the same trend with time. As the hydraulic fracture approaches, the stress at the intersection point gradually changes from compressive stress to tensile stress, and the tensile stress is at 40.85s and 33.95s, respectively. It reached the peak value of 8.58MPa and 8.86MPa, and then began to decrease; Fig. 15(b) is the comparison curve of shear stress at the intersection point. The experimenter can see the shear stress at the intersection point in the fracturing example of highly deviated well during the entire hydraulic fracture propagation process. It is obviously larger than that of the horizontal well fracturing example, in which the shear stress at the intersection points in the horizontal well example is almost 0, and the force dominated by tensile stress fails to pass through the second interface. In contrast, in the example of the highly deviated well, the shear stress reaches 1.5MPa at 33.95s, and the failure at the intersection is the result of the combined action of tensile stress and shear stress, that is, the second interface is more easily destroyed under the combined action of tensile and shear stress. Penetration to achieve connectivity between reservoirs.

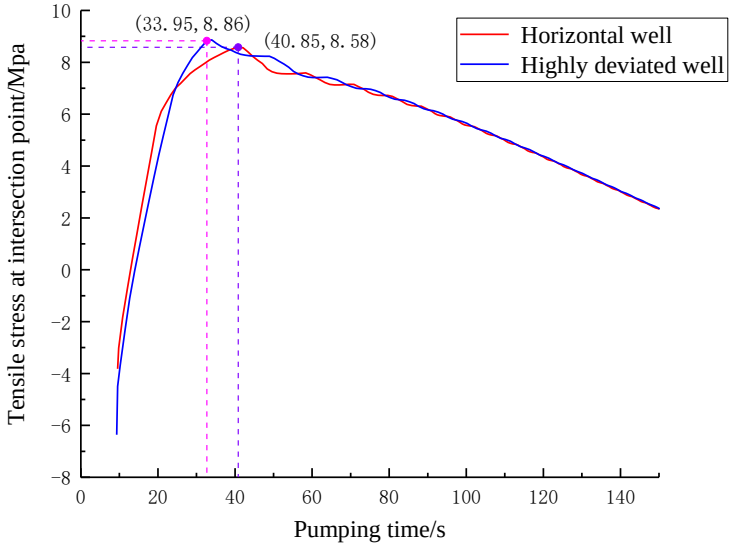

(a)Tensile stress-time curve.

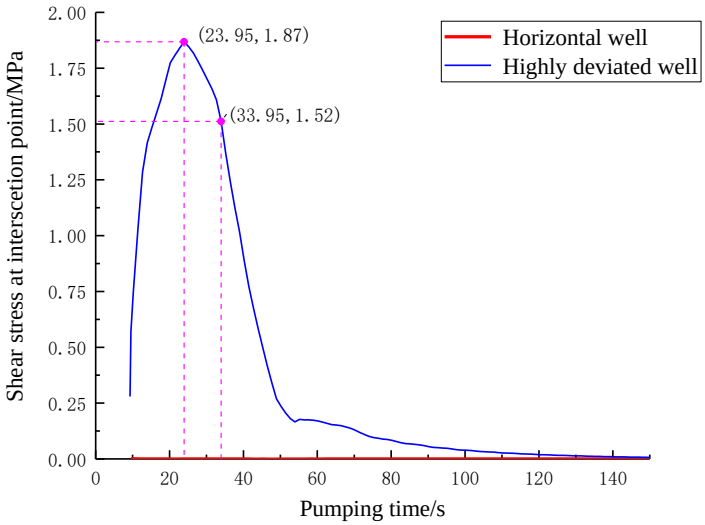

(b)Shear stress-time curve.

Fig 15. Stress-time curve of horizontal wells and highly deviated wells.

The experimenter further analyzed the change mechanism at the intersection of the horizontal well and the highly deviated well. The experimenter extracted the vertical displacement at the time of failure at the intersection of the horizontal well and the highly deviated well (Fig. 16). The vertical displacement of the well is significantly larger than that of the horizontal well. At this time, the displacement of the highly deviated well shows that the left side of the middle layer moves down near the fracture area, and the right side near the fracture area moves up, which causes shear stress in the thin interlayer. With symmetrical boundary conditions, there is no obvious vertical displacement in the middle layer, the vertical displacement is symmetrically distributed, and there is no relative displacement on the left and right sides of the hydraulic fracture, so there is no obvious shear stress at the intersection. For highly deviated wells, the fractures start to expand, and the direction is gradually deflected to the direction of vertical in-situ stress. The fractures form a structure similar to an inclined fault, which causes the rock masses on both sides of the fracture to slip relatively under the action of vertical in-situ stress. As the hydraulic fracture continues to expand, the relative slip of the rock mass on both sides increases continuously, and the shear stress on the thin interlayer increases. Finally, the thin interlayer is penetrated by the tensioning action of hydraulic fractures and the shearing action of relative slip.

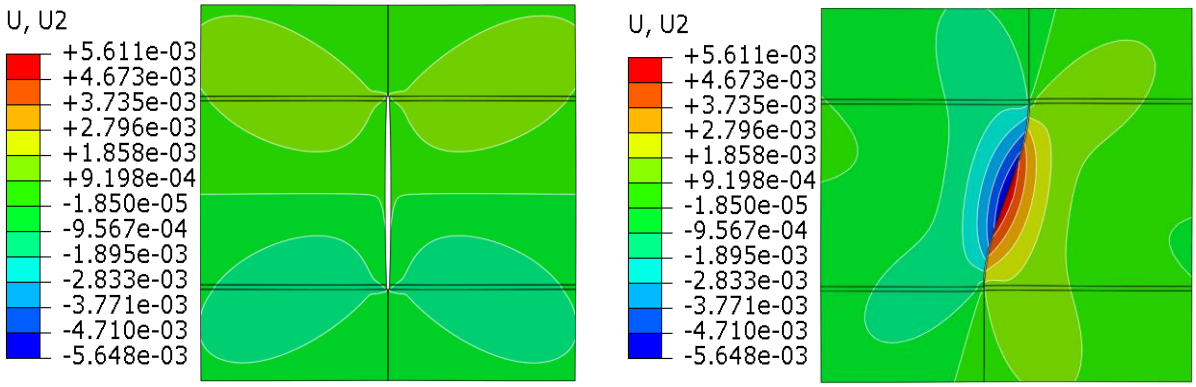

(a)Vertical displacement of horizontal well (b)Vertical displacement of highly deviated well

Fig 16. Vertical displacement comparison between horizontal well and highly deviated well.

4. Conclusion

In this paper, taking the Changqing Oilfield No. 6 reservoir development project of Huaqing Oilfield as the background, this paper studies the problem that the fracturing effect of highly deviated

wells is better than that of horizontal wells. In this paper, fracturing samples containing thin interlayers are carried out. In the physical model test, the cohesion element is used to numerically simulate the interaction behavior of hydraulic fractures and thin interlayers under different well types. This paper draws the following conclusions:

1. The stimulation mechanism of highly deviated wells is: under the same in-situ stress conditions, highly deviated wells are easier to penetrate the thin interlayer interface than horizontal wells, and highly deviated wells communicate with adjacent reservoirs, so the reservoir stimulation range is wider It is easier to achieve production stimulation than horizontal wells.

2. When the experimenters use highly deviated wells for fracturing, the failure of the thin interlayer is the result of the combined action of tensile stress and shear stress, while the thin interlayer is only affected by tensile stress under the condition of horizontal wells, so the highly deviated well Hydraulic fractures are more likely to penetrate thin interlayers during fracturing.

3. The deflection and extension of hydraulic fractures in highly deviated wells make the intermediate reservoirs form a structure similar to inclined faults. Under the action of vertical normal stress, the rock masses on both sides of the fractures undergo shear slippage, and the thin interlayers are subjected to shearing action. With the expansion of the fracture, the sliding amount of the rock mass on both sides continues to increase, and the thin interlayer is finally penetrated by the tension and slip shear of the hydraulic fracture.

Acknowledgments

This work was supported by Hubei Provincial Natural Science Foundation of China (Grant No. 2020CFB367).

References

[1] Du Xianfei, Li Jianshan, Qi Yin, et al. multi-stage fracturing technology for inclined wells in tight and thick oil layers. Petroleum Drilling and Production Technology, 2012, 34(04): 61-63. (In Chinese)

[2] Wang Chengwang, Fan Wenmin, Lu Hongjun. Research and application of production and injection technology for old wells in Changqing Oilfield. Oil and Gas Well Testing, 2007(06):63-67+75. (In Chinese)

[3] Liu Z, Jin Y, Chen M, et al. Analysis of non-planar multi-fracture propagation from layered formation inclined-well hydraulic fracturing. Rock Mechanics and Rock Engineering, 2016; 49(5): 1—12.

[4] Wang, J-J., and R.J. Clifton. "Fracture Growth in the Presence of Highly Stressed Layers." Paper presented at the SPE Western Regional Meeting, Long Beach, California, and March 1991.

[5] Simonson E R, Abou-Sayed an S, Clifton R J. Containment of massive hydraulic fractures. Society of Petroleum Engineering of AIME.

[6] Gao Jie, Hou Bing, Tan Peng. Mechanism of hydraulic fracture propagation through interlayer of sand-coal interbed. Journal of Coal Industry, 2017, 42(S2): 428-433. (In Chinese)

[7] Hou Bing, Chen Mian, Diao Ce, et al. A true triaxial experimental study of fracture propagation through directional wells in sand-mud interaction reservoirs. Science, Technology and Engineering, 2015, 15(26): 54- 59. (in Chinese)

[8] Biot. M A, Medlin W L, Masse L. Fracture Penetration through an Interface. SPEJ, 1983, 23(6):857-869.

[9] Yang Zhaozhong, Zhang Dan, Yi Liangping, Li Xiaogang, Li Yu. Model and Numerical Simulation of Longitudinal Propagation of Fractures in Multi-layer Stacked Coal Seams [J/OL]. Coal Journal: 1-12[2021-03-13]. https://doi.org/10.13225/j.cnki.jccs.2020.1261.

[10] Llanos, E.M. Jeffrey, R.G. Hillis, R. et al. Hydraulic Fracture Propagation through an Orthogonal Discontinuity: A Laboratory, Analytical and Numerical Study. Rock Mech Rock Eng 50, 2101–2118 (2017).

[11] Renshaw. C. E. Pollard DD An experimentally verified criterion for propagation across unbounded frictional interfaces in brittle, linear elastic materials. International Journal of Rock Mechanics and Mining Sciences & Geomechanics Abstracts, 1995. 32(3) :237-249

[12] Pan Rui, Zhang Guangqing. Research on the influence of layered rock fracture energy anisotropy on the propagation path of hydraulic fractures. Chinese Journal of Rock Mechanics and Engineering, 2018, 37(10): 2309-2318.

[13] Pan Rui, Zhang Guangqing, The influence of fracturing energy anisotropy on hydraulic fracturing path in layered rocks. Chinese Journal of Rock Mechanics and Engineering, 2018, 37(10):2309-2318.

[14] Huang Rongzun. The initiation and propagation of hydraulic fracturing fractures. . Petroleum Exploration and Development, 1981(05):62-74. (In Chinese)

[15] Daneshy.A.A. Hydraulic fracture propagation in layered formationsJ]. Society of Petroleum Engineers Journal, 1978, 18(1): 33-41.

[16] Gao Jie, Hou Bing, Chen Mian, et al. Effects of lithologic differences and interface properties on fracture initiation and propagation. Chinese Journal of Rock Mechanics and Engineering, 2018, 37(S2): 4108-4114. (In Chinese)

[17] Anderson, G. D. Effects of Friction on Hydraulic Fracture Growth near Unbonded Interfaces in Rocks. Society of Petroleum Engineers. 1981.21(1):21-29.

[18] Teufel, L. W., & Clark, J. A. Hydraulic Fracture Propagation in Layered Rock: Experimental Studies of Fracture Containment. Society of Petroleum Engineers. 1984.24(1):19-32.

[19] Guo Yintong, YANG Chunhe, Jia Changgui, et al. Research on hydraulic fracturing physical simulation of shale and fracture characterization methods. Chinese Journal of Rock Mechanics and Engineering, 2014, 33(1): 52–59. (In Chinese)

[20] Heng Shuai, Yang Chunhe, Zeng Jinyi, et al. Experimental study on hydraulic fracture geometry of shale. Chinese Journal of Rock Mechanics and Engineering, 2014, 36(07):1243-1251. (In Chinese)

[21] Detournay, Emmanuel. Propagation Regimes of Fluid-Driven Fractures in Impermeable Rocks. International Journal of Geomechanics. 2004. 4(1):35-45.

[22] Chen Ming, Zhang Shicheng, Xu Yun, etc. Boundary element model of interaction between hydraulic fractures and natural fractures based on complementary algorithm. Chinese Journal of Rock Mechanics and Engineering, 2018, 37(S2): 3947-3957.